2022

Investigating the role of the tight junction protein claudin-4 in experimental IBD

https://hdl.handle.net/2144/45601

BOSTON UNIVERSITY

SCHOOL OF MEDICINE

Thesis

INVESTIGATING THE ROLE OF THE TIGHT JUNCTION PROTEIN CLAUDIN-

4 IN EXPERIMENTAL IBD

by

YUNUO LIU

B.A., Boston University, 2020

Submitted in partial fulfillment of the

requirements for the degree of

Master of Science

2022

Approved by

First Reader   _____
               Mina Moussavi, Ph.D.
               Assistant Professor of Physiology and Biophysics

Second Reader   _____
               Nitesh Shashikanth, Ph.D.
               Postdoctoral Fellow
               Brigham and Women's Hospital

Third Reader   _____
               Jerrold R Turner, Ph.D., M.D.
               Professor of Pathology
               Harvard University, School of Medicine

ACKNOWLEDGMENTS

INVESTIGATING THE ROLE OF THE TIGHT JUNCTION PROTEIN CLAUDIN-4 IN EXPERIMENTAL IBD

YUNUO LIU

ABSTRACT

Intestinal bowel disease (IBD) comprises several chronic disorders that can cause inflammation in the intestines. Defects in the epithelial barrier function have been observed to play a vital role in IBD pathology. Claudins are a family of integral membrane proteins that comprise tight junctions and are critical determinants of epithelial barrier function. The pore-forming claudins regulate paracellular flux by forming charge and size-selective pores, e.g., claudin-2 and -15. On the other hand, so-called barrier-forming claudins, such as claudin-4, are supposed to function by forming a fence/seal at tight junctions. Previous studies have shown that unregulated paracellular permeability in mice overexpressing a pore-forming claudin-2 results in severe clinical disease in an experimental IBD model, whereas claudin-2 KO mice are protected. However, the role of barrier-forming claudins like claudin-4 in an experimental IBD setting has not been well examined. In this study, two kinds of experimental IBD models- chronic (T cell transfer) and acute (DSS) models to study IBD in mice. As claudin-4 is a barrier-forming claudin, we hypothesized that conditional claudin-4 knockout promotes intestinal damage and induces colitis. Surprisingly, we found that claudin0-4 KKO had a protective effect on the disease severity compared to WT or claudin-4 overexpressing transgenic mice. These results show that the tight junction barrier

enhancing functions of claudin-4 might be secondary to its effect on epithelial wound repair.

TABLE OF CONTENTS

LIST OF TABLES

LIST OF FIGURES

LIST OF ABBREVIATIONS

AT	Adoptive Transfer
BCH	Boston Children's Hospital
BWH	Brigham and Women's Hospital
CBC	crypt base columnar
CD	Crohn's disease
CLDN4	Claudin-4
CPE	Clostridium perfringens enterotoxin
DSS	Dextran sodium sulfate
ECL1	first extracellular loop
EDTA	Ethylenediamine tetraacetic acid
FACS	fluorescence-activated single cell sorting
FOBT	Fecal Occult Blood Test
Foxp3	scurfin
FRT	flippase recognition target
GATA3	GATA Binding Protein 3
GFP	green fluorescent protein
GWAS	Genome-Wide Association Studies
HBSS	Hank's balanced salt solution
IBD	Inflammatory bowel disease
IEC	Intestinal epithelial cell
IFN-γ	Interferon gamma

IL-6/-13/17a/-33	Interleukin-6/-13/-17a/-33
JAM-A	Junctional adhesion molecule A
kDA	kilodaltons
KO	Knockout mouse
Lgr5+	Leucine Rich Repeat Containing G Protein-Coupled Receptor 5
loxP	Locus of Crossover in P1
LPL	Lamina propria lymphocytes
MDCK-II	Madin-Darby canine kidney
MLC	myosin light-chain
MLCK	myosin light chain kinase
Na^+/K^+ ATPase	sodium–potassium pump
OLFM4+	Olfactomedin 4
PAMR	perijunctional actomyosin ring
PCR	Polymerase Chain Reaction
PDZ	post synaptic density protein, Drosophila disc large tumor suppressor, and zonula occludens-1 protein
PGK	Phosphoglycerine Kinase
PMA	Phorbol 12-myristate 13-acetate
RPMI	Roswell Park Memorial Institute Medium
SGLT1	sodium glucose cotransporter
ST2	Interleukin 1 receptor-like 1/ IL-33 receptor

Tg	Transgenic mouse
Th1/2	T helper type 1/ type 2
TNBS	Trinitrobenzenesulfonic Acid
TNF-α	Tumor necrosis factor alpha
UC	ulcerative colitis
WT	Wild-type mouse
ZO1/2	Zonula occludens-1/-2

INTRODUCTION

The intestine is tasked with absorbing nutrients from digested food while simultaneously providing a barrier to luminal pathogens and toxins, preventing them from entering the body. As described below, nutrient absorption and barrier function are integrated.

Understanding these routes and how they interact is clinically relevant, as regulatory failures have been linked to various intestinal pathologies in humans [1-3]. Furthermore, this knowledge is essential for generating novel therapies designed to combat barrier dysfunction in gastrointestinal diseases, including Crohn's disease (CD) and ulcerative colitis (UC), the two primary forms of inflammatory bowel disease (IBD) that significantly reduce the quality of life in patients [4-9].

Anatomy of the intestinal mucosa

The intestinal mucosa is a multilayered barrier lined by columnar epithelial cells. This epithelial cell population is heterogeneous, and different cell types have different functional roles in maintaining intestinal homeostasis [10]. In the base of the crypt, crypt base columnar (CBC) cells (Lgr5^{+}, OLFM4^{+}, Msi1^{+}) can be found in between Paneth cells. The CBC cells are fast-cycling cells that are thought to be the significant stem cell population within the intestine, and single Lgr5^{+} cells have been shown to give rise to heterogeneous crypt organoids in vitro [11]. Lgr5^{+} CBCs can undergo self-renewal to maintain the CBC population

and give rise to transient amplifying cells, proliferative progenitors that differentiate into mature intestinal epithelial cell types. During maturation, cells migrate out from the crypt, and this process is due to both mitotic pressure and active migration. Another population of label-retaining cells can be found in the +4 position above the paneth cells. Evidence shows that this slow-cycling stem cell population is required for intestinal regeneration after injury [12].

Transient amplifying progenitor cells produced from Lgr5$^+$ CBCs differentiate into at least five mature intestine epithelial cells, including paneth, enteroendocrine, goblet, enterocyte, and tuft cells [13]. Each cell type migrates away from the crypt to cover the villi, except paneth cells, which migrate into the crypts and secrete different growth factors and antimicrobials [14]. Enterocytes are absorptive cells that compose most of the intestinal epithelium (~90%) [13]. Goblet cells, the next most common cell type (~10%), secrete mucins that form a gel-like substance that composes an unstirred layer, preventing intestinal bacteria from directly contacting the epithelial surface [15-17]. Enteroendocrine cells secrete hormones that regulate digestive processes. Finally, tuft cells, a scarce cell population in intestine villi, represent approximately 0.5% of the intestinal epithelial cells. Tuft cells were identified decades ago, but only recent research has discovered their crucial role in immune type 2 responses to helminth infection and secreting IL-25 [16, 18-22]. Beneath the intestinal epithelia, there is a space called the lamina propria, which contains blood vessels and lymphatic vessels. Nutrients absorbed by the intestine by either transcellular

or paracellular absorption enter the lamina propria, which can be absorbed into the blood.
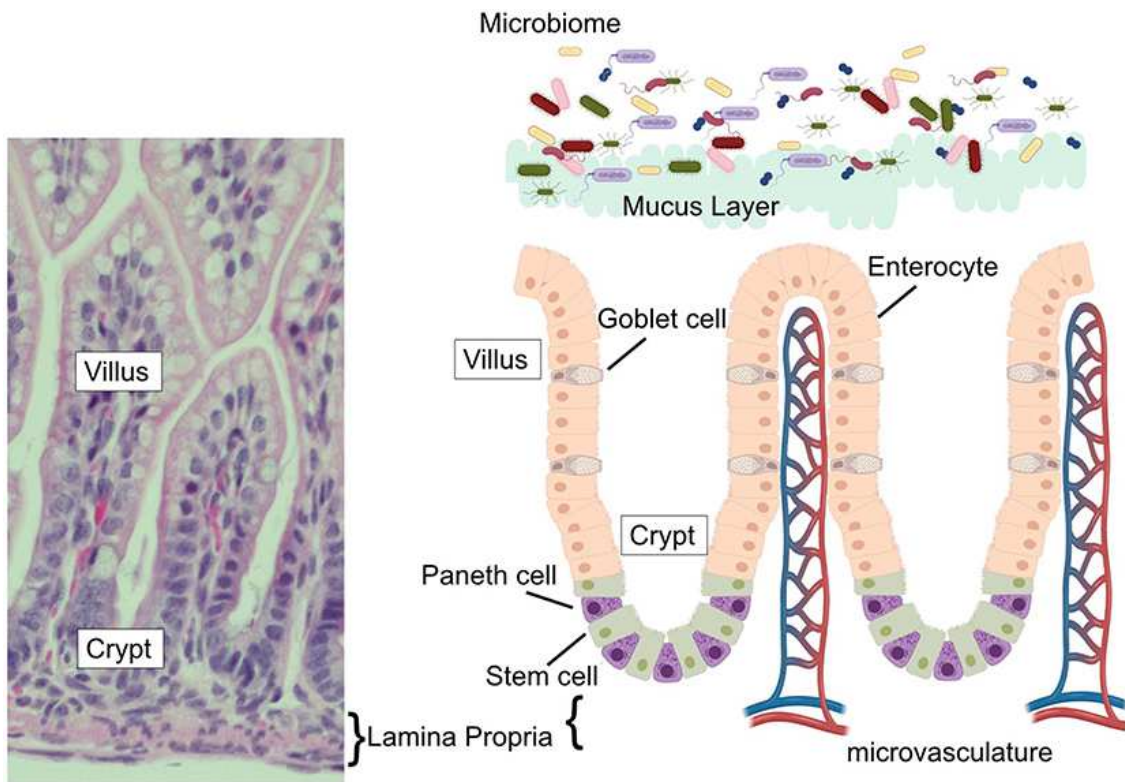

Figure 1. The intestinal epithelium. This figure shows the different cells of intestinal epithelium [23].

Different routes for nutrient absorption in the intestine

In order to facilitate life, the intestine must selectively absorb nutrients from digested food while at the same time establishing a selective barrier preventing microorganisms and toxins from entering the body [24]. This phenomenon is termed transepithelial transport, which can occur by two major routes: paracellularly, in which the nutrients pass through the junctions between epithelial cells, and transcellular, where nutrients are first selectively internalized by the epithelial cells by transporter proteins on the apical surface of the epithelium, before being further transported into the lamina propria by basolateral transporters [25].

Transcellular pathway

The transcellular pathway consists of channel and transporter proteins that allow bidirectional transport between the lumen and lamina propria [10]. Some transporters are located on the apical cell surface and facilitate nutrient absorption by the intestine epithelia. Other proteins are located on the basolateral surface and allow nutrients to exit the epithelial barrier into the lamina propria to be absorbed by the blood or lymphatic system. Different transmembrane transporters have different mechanisms for a different specific cargo. For example, glucose absorption in the intestine occurs primarily through the sodium-glucose cotransporter (SGLT1), which facilitates glucose transport by coupling it with the energetically favorable entry of sodium into intestinal epithelial

cells [26, 27]. This process is dependent on maintaining a low intracellular concentration of sodium, a feat accomplished by a basolateral membrane transporter called the Na^+/K^+ ATPase. This ATP-powered pump facilitates the exchange of three Na^+ for two extracellular K^+ [28]. Therefore, the transcellular transport pathway operates by apical and basolateral transport proteins. Intestinal epithelial cells must actively maintain the correct localization of these transport proteins to different plasma membrane domains to allow for transcellular transport function.

Paracellular pathway

The route taken by different nutrients is determined by the size, charge, and availability of specialized transmembrane protein transporters available for each nutrient. While the routes and nutrients targeted by each pathway are different, overall, the activity of each pathway plays a critical role in regulating the function of the other. The paracellular transport pathway is defined as the passive transepithelial transport that occurs when molecules, including water, sodium, and other solutes, cross between adjacent intestinal epithelial cells to enter the lamina propria without being internalized by the epithelial cells [29]. This pathway can be further refined into the pore pathway- composed of pores found in tight junctions that allow for size-selective and charge-selective facilitated diffusion, and the leak pathway that allows the passage of larger molecules [30]. Larger molecules and components of the microbiota may also

cross the epithelial layer when damaged through ulceration and erosion

processes, utilizing an unrestricted pathway [2, 31]. Each of these paracellular

transport pathways is described in more detail below:

Pore pathway

The pore pathway transports small molecules smaller than 8 Å in

diameter, including water, glucose, and selectively charged/uncharged molecules

[32]. Pores are located in tight junctions and have been shown to be composed

of claudin proteins [33]. Claudins have been shown to play essential roles in

regulating tissue permeability in the intestine, skin, and kidney [10, 34, 35]. Early

investigations into claudin proteins focused on how their expression regulated the

electrical resistance and permeability of epithelial monolayers to small ions

across entire epithelial sheets, primarily due to the inability to investigate

individual channels. For example, while claudin-dependent channels were

previously thought to be similar to constantly open passages, patch clamping

single channels have demonstrated at least three different channel

conformations (including two gated positions and one open position). This finding

suggests that gating of claudins might serve as a regulatory mechanism, but the

factors that regulate channel conformation have yet to be identified.

Leak pathway

Unlike the pore pathway, the exact location of paracellular transport occurring via the leak pathway, which transports molecules with a maximum diameter of 100 Å, remains unclear. It has been theorized that leakiness can occur due to the dynamic nature of tight junctions [36]. Alternatively, macromolecules might pass at junctional sites of contact from three epithelial cells, which form a central tube that has been shown to be negatively regulated by the tricellulin expression [37].

Although the exact path that macromolecules take to pass the barrier has yet to be elucidated, a great deal is known about regulators of leak pathway function. The phosphorylation of myosin light-chain (MLC), a component of the perijunctional actomyosin ring (PAMR), has been shown to increase the passage of nutrients [2, 38-40]. In addition, occludin has been shown to regulate the paracellular ion conductance and maintain the cation-selective barrier [41]. Later work determined that cytokines, including IFN-γ and TNF-α, which reduced intestinal barrier function, act by stimulating the myosin light chain kinase (MLCK) [42].

Unrestricted pathway

A third paracellular route called the unrestricted pathway, which does not restrict the size of substances crossing the epithelial barrier of the intestine, can occur when the epithelial barrier becomes physically damaged. Damage to the

intestinal epithelium results from several distinct (although related) mechanisms, including T-cell mediated tissue damage and ulcerations [2]. These different damage mechanisms often result from inflammatory conditions found in patients with intestinal pathologies that are broadly described as inflammatory bowel disease (IBD), which result in loss of barrier function [4, 43]. In the culture of MDCK-II cells, the unrestricted pathway can be re-capitulated by knocking down ZO1/2, eliminating tight junction structures, or by simultaneously deleting five different claudin paralogs and JAM-A [43, 44]. Barrier damage may also be modeled in animals by applying cytotoxic agents, including DSS and TNBS [45, 46].
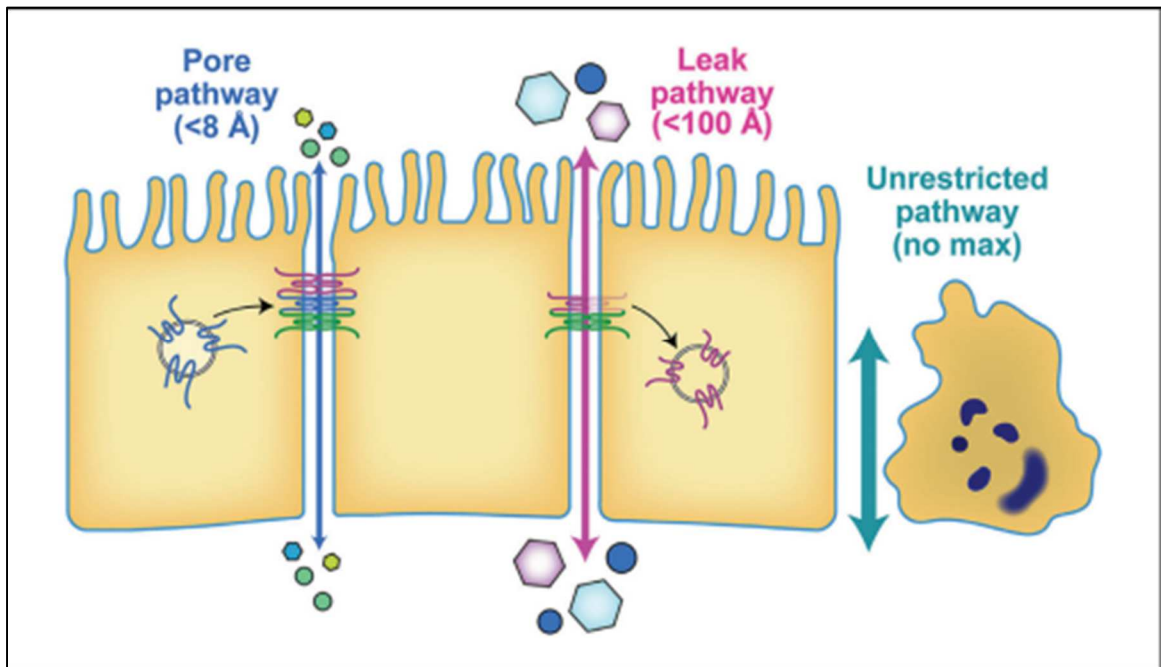

Figure 2. Routes of absorption. This figure shows the difference between the paracellular pathways [47].

Claudin

The 27 human claudin proteins have different functions; some form pores in tight junctions, while others have a gating function. Pore-forming claudins may be further subdivided by their preference for the charge of the ions they transport [33, 48-50]. They are a major structural component of tight junctions.

Structurally, claudins are a family of transmembrane proteins with intracellular N and C terminus with four transmembrane helices and two extracellular segments. These tetraspanning membrane tight junction proteins form two extracellular segments, consisting primarily of β-sheets with select amino acid residues found in the first extracellular loop that convey charge selectivity to different claudins [51-55]. The first extracellular loop (ECL1) is a highly conserved motif of claudins. In the second half of the ECL1, claudin-2 and claudin-15 have specific charged residues responsible for determining the charge selectivity [56].

After the second conserved extracellular cysteine (C64), mutations of charge residues can alter charge selectivity for claudin-2, -10a, etc. [56-59]. ECL1 also has a pair of conserved extracellular cysteine 9-11 residues after the G-L-W motif. There is also a highly conserved arginine at the end of ECL found in 23 claudins [60]. Studies have found that toxins such as Clostridium perfringens enterotoxin (CPE) have been found to induce claudin internalization. The effect of CPE in claudin-3 and claudin-4 is due to direct interaction with the ECL2 and forms pores in the membrane to induce cell death [61, 62]. The

cytoplasmic tail plays a role in trafficking to the tight junction, protein degradation,

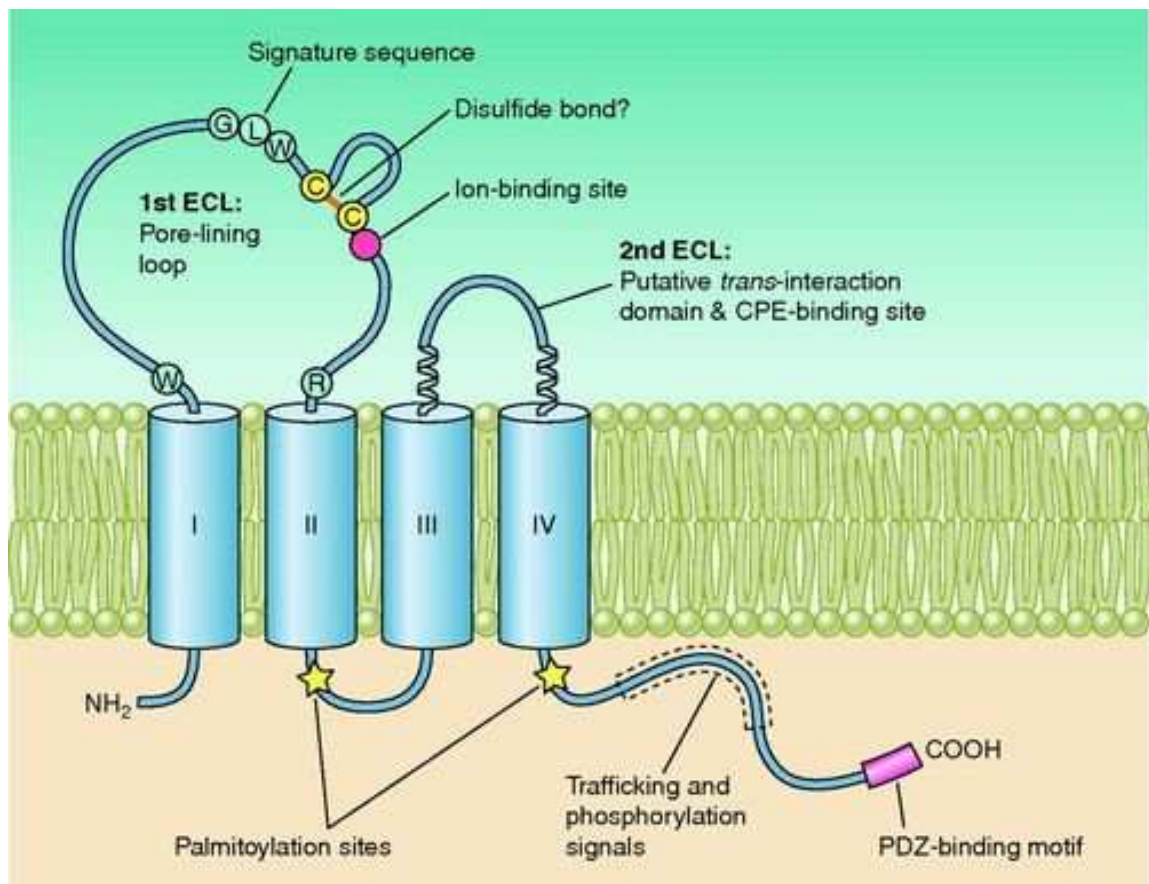palmitoylation, and phosphorylation and binds to the PDZ domain [60].

Figure 3. Structure of a claudin protein. This figure describes the different parts of the structure of a generic claudin protein [60].

All claudins have C-terminal PDZ binding motifs that enable direct interaction with tight junction cytoplasmic proteins. Claudins can interact with the cytoplasmic scaffolding proteins such as ZO-1 and ZO-2, indirectly linking claudins to the actin cytoskeleton. Claudins can be distinguished into pore-forming or barrier-forming claudins. Pore-forming claudins increase the paracellular permeability for ions of different sizes and charges, such as claudin-2, -10b, and -15 as cation pores and -10a and -17 as anion pores [60].

Claudins can be found in all epithelial tissues. In the kidney, tight junction proteins can be found in the glomerulus, podocytes, Bowman's capsule, etc. The more notable claudin-2, claudin-10a, and claudin-17 can be found in the proximal tubules [58, 63-65]. In the liver, claudin-1 is expressed in hepatocytes and the bile duct, while claudin-4 is not detected [60]. Claudins can be found in different regions of the small intestine and colon in the intestine. Some are restricted to the tight junction, and others, such as claudin-4, are also found along the basolateral membrane [66-69]. Claudin expressions also vary with development. Claudin-2 is expressed at high levels at birth but gradually decreases, whereas claudin-3, -4, -7, and -15 increase during early life towards adulthood [69].

Overexpression of pore-forming claudins can increase permeability to cations or anions, and barrier-forming claudins can decrease permeability to cations or anions such as claudin-4 decreases permeability to cations when overexpressed [60]. Claudin-2 overexpression increases paracellular Na^+ and water permeability [70].

IBD

Although the exact cause of IBD is not determined, several factors are closely linked to IBD, such as microbiota dysbiosis, obesity, genetic factors, age, and ethnicity.

Crohn's disease (CD) and ulcerative colitis (UC) are two major types of inflammatory bowel disease (IBD). UC is limited to the proximal, distal colon, and rectum, whereas the entire intestinal tract can be infected with CD.

Interestingly, defects in the intestinal barrier have also been reported in 10% of healthy relatives of IBD patients [71-75]. This finding suggests an underlying genetic component for IBD that allows for the passage of antigens through the intestinal epithelia, promoting an immune response. Another GWAS study was specifically designed to identify gut permeability loci by comparing healthy relatives of IBD patients with greater levels of intestinal permeability to control individuals exhibiting normal barrier function. However, this study failed to yield significant targets [71].

Ulcerative colitis

Ulcerative colitis is one of the significant chronic IBD caused by inflammation and ulcers on the colon's inner lining. Ulcerative colitis usually occurs in the large intestine and rectum. Unlike Crohn's disease, the damaged areas in UC are usually continuous and affect the innermost lining of the intestine.

Studies have shown that claudin-1, a barrier-forming claudin level, increases in the colon of UC patients [76], but the expression depends on the severity of the inflammation [77]. Other studies have shown that claudin-2 level increases, and claudin-3, -4, and -7 decrease in ulcerative colitis [78].

Crohn's Disease

Crohn's disease can affect any area in the digestive tract from mouth to anus, but mainly in the small intestine and colon. The damage caused in the intestine can appear patchy with areas of healthy tissue, and it can reach through multiple layers of the GI tract.

Diminished tight junction strands can also be found in CD patients. Claudin-2 expression increased three-fold in duodenum and colon [79, 80]. CD exhibits a Th1 immune response which is different from UC cases. The claudin-2 expression is upregulated by TNF-α and interferon-gamma [79, 81]. Claudin-4 is not changed in the tight junction, but decreased in the duodenum [79, 80]. Claudin-5 and -8 expressions are downregulated in tight junctions [79]. Further investigations revealed increased expression of the pore-forming claudin-2, accompanied by decreased expression and altered distributions of barrier-forming claudin-5 and -8, were associated with Crohn's [82].

TIGHT JUNCTION CLAUDINS AND IBD

Tight junction proteins are affected in several other intestinal diseases like celiac disease and irritable bowel syndrome. Claudin-2 and claudin-15, two pore-forming claudins, have been shown to increase celiac disease [83].

Human data suggested a link between claudin-2 mediated intestinal permeability and IBD, which can be characterized by an increase in the concentration of inflammatory cytokines, including IL-13. However, the mechanism connecting these complicated biological processes remained obscure. In order to unravel how they might be connected, Raju et al. recently tested the consequences of claudin-2 overexpression and claudin-2 inactivation in the murine immune-mediated colitis model [84]. Using the claudin-2 KO model, the authors demonstrate that the production of IL-13 is directly correlated with claudin-2 expression and that claudin-2 KO mice were protected from the loss in barrier function observed in WT mice after IL-13 injection.

Claudin-2 overexpression can also be found in inflamed tissue and is upregulated by cytokines such as IL-33, TNF-α, and IL-6, which are involved in the Th2 immune response [85]. In the renal biopsies, claudin-4 expression is decreased, and it may contribute to impaired epithelial barrier function [86].

Experimental models of IBD

There have been several different ways of studying IBD, such as clinical studies, in vitro, and in vivo models. Although clinical studies are suitable for

better representation of IBD in humans, there are not enough to understand the mechanisms behind IBD. On the other hand, in vitro experiments are great for mechanisms, but they cannot replicate in vivo experiments. Mouse models are more widely used because of the different ways to modify the models to represent different levels of disease. Although not perfect, we can use models that can relatively closely represent human IBD.

DSS

DSS is dextran sodium sulfate that can be administered in water to induce reversible colitis in mice. Dextran sodium sulfate is a harmful detergent that will create acute tissue inflammation, mainly in the colon. It mimics the pathology of ulcerative colitis, which is an effective form of intestinal bowel disease [87]. DSS model is popular due to its rapidity, reproducibility, and controllability. DSS concentrations and the frequency of administration can be modified for acute and chronic models [88]. 5% DSS (usually 1-3%) in water is usually given to the mice for up to 10 days, and it usually takes around seven to nine days to induce colitis.

Adoptive transfer

The Rag1KO mice have significantly fewer T and B lymphocytes than the wild-type mice. Since chronic inflammation of the intestine is mediated by T cells, colitis can be induced chronically by the adoptive transfer of 5 x 105 purified CD4+CD45Rbhi lymphocytes (naïve T cells) from healthy wild-type mice into

immune-deficient Rag1 KO mice around 4-8 weeks after T cell transfer [89, 90]. The significant advantages of this model are that one can examine the very earliest immunological events associated with the induction of gut inflammation and the perpetuation of disease [91].

SPECIFIC AIMS

In this study, Chronic (T cell transfer) and acute (DSS) model to study IBD in mice. As claudin-4 is known as a barrier forming claudin, we hypothesized that conditional claudin-4 knockout promotes intestinal damage and induce colitis.

METHODS

Mice

All experiments used C57BL/6 mice bred and maintained at Boston Children's Hospital in accordance with BWH and BCH Institutional Animal Care and Use Committee regulations. The donor mice (Stock.002216) used in the AT model are purchased from Jackson Laboratory (Bar Harbor ME). All mice in the DSS model were 8-9 weeks old at the start of the experiment and 10-11 weeks old in the AT model.

CLDN4$^{IEC.KO}$

A targeting vector with exon 1 of human claudin-4 flanked by two loxp sites and a PGK-neo expression cassette flanked by two FRT sites is inserted into the target WT locus between the mice claudin-4 gene. The flp enzyme removed the PGK cassette after correctly targeting it. The mice are backcrossed to get homozygous flox mice eventually. Then the mice are bred with a cre expressing mouse to produce flox mice with cre [92]
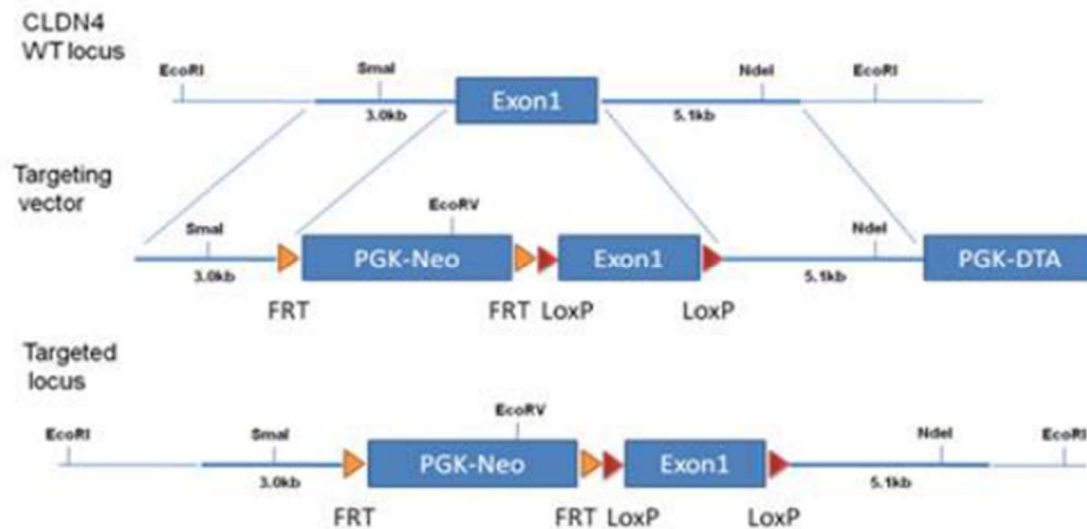
Figure 4. CLDN4^{WT} locus with the targeting vector and target locus.
Note. Adapted from Gong Y's proc Natl Acad Sci paper [92].

CLDN4^{Tg}

To make the claudin-4 transgenic mice, we created a transgenic construct
with promoters, introns, cDNA of claudin-4, poly-A site, and a reporter gene for
mcherry, a red fluorescent protein. We microinjected a plasmid containing the
gene construct into embryonic stem cells and then injected it into mouse
blastocysts. This caused non-homologous recombination that incorporated the
DNA randomly into the mouse genome. After using multiple PCR primers to
detect the Tg gene band, we bred them with CLDN4^{WT} mice to create the
transgenic mice line.

DSS model

For the majority of the studies, we gave 1-3% (wt/vol) DSS (molecular weight 40 kD) in water for seven to nine days to induce colitis.

In the DSS experiment that lasted 25 days, 2% DSS was given for nine days, and then we replaced the DSS with water and continued to monitor the mice for recovery for up to 25 days.

Control C57BL/6 mice received the same water without the DSS for the duration of the experiment. All water and DSS are changed every other day. All mice were monitored and sacrificed at the humane endpoint of the experiment. Then all the mice were sacrificed for tissue collection, RNA and protein analysis, and LPL isolation, as described below.

We measure the weight loss every day with DSS in water, and after replacement of DSS with water, we measure the weight loss every 2-3 days. For disease severity, we followed the same scoring system as the DSS model listed in table 1.

AT model

The spleen from donor mice is harvested and ground over 70 um filter in cold PBS to isolate the lymphocytes. After centrifugation, MACs buffer is added to lyse red blood cells at room temp. The cells are filtered through a 40 µm filter and counted 10 X 105 unpurified cells to purify with the Miltenyi naive T cell

isolation kit. CD4+ splenocytes are isolated by magnetic-activated cell sorting beads (Miltenyi Biotec) and LS columns (Miltenyi).

Isolated lymphocytes will be injected into mice by retro-orbital injection. We measured the weight loss every 3 to 5 days, and with increased disease severity, we monitored and weighed the mice every two days. For disease severity, we followed the same scoring system as the DSS model listed in table 1.

Control Rago1 KO mice did not receive naïve T cells at the start of the experiment. All mice were monitored and sacrificed at the humane endpoint of the experiment. Then all the mice were sacrificed for tissue collection, RNA, and protein analysis.

Clinical scoring

For disease severity, we measured the score from 0 to 3 based on fur, posture, activity, stool consistency, and presence of blood in the stool. The detailed scoring is listed in table 1. We combined all the scores for each mouse every day to get a comprehensive clinical score for disease severity.

LPL isolation

Colon was harvested and then put into 2% FCS/HBSS to flush. We removed any fat tissue and Peyer's patches. The intestine is then cut and incubated with two mM EDTA/HBSS for 30 minutes. The tissue samples are

filtered and washed with HBSS. The tissue samples are then incubated with two mM EDTA/HBSS for 15 minutes and washed with 1X HBSS. Tissue segments are incubated in complete RPMI media with collagenase VIII (Sigma) and Dnase 1 (Sigma) in complete LP Th17 or RPMI, which included 10% FBS, 1.5 % HEPES, No essential aa 1%, and pen/strip 1%. FACS buffer (1X PBS, 2% FBS, 2mM EDTA) is added to the enzyme mix and passed single-cell suspension through a 70 µm cell strainer. After centrifugation and resuspension with FACS buffer, passed single-cell suspension again with 40 µm cell strainer to centrifuge and resuspended with RPMI media. We then plated the cells into 24 well-plate for cytokine induction with media containing PMA (Sigma), Ionomycin calcium (Sigma), and Golgi plug (BD) for 3.5 hours.

Flow cytometry staining/analysis

The cells are stained with blocking antibody CD16/CD32 and incubated for 10 min. Then it is stained for CD25. CD3, live/dead, CD4, ST2 receptor and CD8 for 30 min. The cells are then fixed with fixation buffer and permeabilization buffer (1:10 dilution, eBioscience) for 5 min each. After fixation, the cells are stained for Il-17a, IFN-γ, Foxp3, and GATA3 for 30 min.

Table. 1. DSS and AT scoring guide.

Parameter	Description	Score
Fur	Smooth, shiny coat (F)	0
	Dull, but flat coat (F)	0
	Dull, slightly pointy (M and F)	1
	Pointy and upright, almost perpendicular to skin	2
Posture	Straight back, no leaning	0
	Slightly but visibly hunched	1
	Hunched a lot as though curved up (will always have problem moving normally)	2
Activity	Normal, running around	0
	Slower in moving, not actively exploring	1
	Hardly moving/moving on cue/looks lethargic	2
	Hyper-active, jumpy and restless, showing signs of delirium	3
Stool Consistency	Hard, break up on spreading	0
	Soft, easier to spread	1
	Very soft, spread easily, still holds up shape	2
	Watery, no shape	3
Stool blood	No sign of FOBT blood	0
	Greenish tinge for positive FOBT	1
	Darker green, but no blue	2
	Blue-ish, signs of darker stool because of occult blood	3
	FOBT+ very blue, visible red blood in stools	4

RESULTS

Chronic colitis experimental model on CLDN4$^{IEC.KO}$ and CLDN4$^{Fl/Fl}$ mice

Claudin-2 has been found to increase disease severity when overexpressed in the T cell transfer experimental model [84]. Barrier forming claudins are supposed to protect tight junctions, such as claudin-1, claudin-4, etc. For example, claudin-1 KO pups die of dehydration [93]. So we hypothesized that knocking out claudin-4 in intestinal epithelial cells of mice will increase disease severity due to its inability to protect and form barriers. To test the hypothesis, I performed adoptive transfer colitis to compare the severity of disease in immune-deficient CLDN4$^{Fl/Fl}$ and CLDN4$^{IEC.KO}$ mice.

Unexpectedly, the significant weight loss of the CLDN4$^{Fl/Fl}$ male mice on day 26 suggests that these mice are more diseased compared to the CLDN4$^{IEC.KO}$ male mice gained weight and had lower clinical scores on day 26 (**Figure 5A**). However, there was no significant difference in disease severity in the CLDN4$^{IEC.KO}$ and CLDN4$^{Fl/Fl}$ female mice. This was demonstrated by the similar weight loss and the clinical scores. Even though the CLDN4$^{IEC.KO}$ female mice had a more significant disease severity within the first week of T cell transfer; as the disease progressed, the CLDN4$^{Fl/Fl}$ mice showed slightly higher disease severity than the CLDN4$^{IEC.KO}$ mice (**Figure 5**). Gross examination showed that, consistent with the increased disease severity, the CLDN4$^{Fl/Fl}$ colon was more inflamed than the CLDN4$^{IEC.KO}$ mice (**Figure 6**). CLDN4$^{Fl/Fl}$ spleens were more inflamed than the CLDN4$^{IEC.KO}$ spleens (**Figure 7**). Overall, these data

indicate that, contrary to our hypothesis, the CLDN4$^{IEC.KO}$ mice did not have increased severity of experimental IBD compared to the CLDN4$^{Fl/Fl}$ mice. Because previous work has shown that increased intestinal permeability by enhancing claudin-2 expression promotes disease progression, these data indicate that claudin-4 KO can function to protect from colitis.
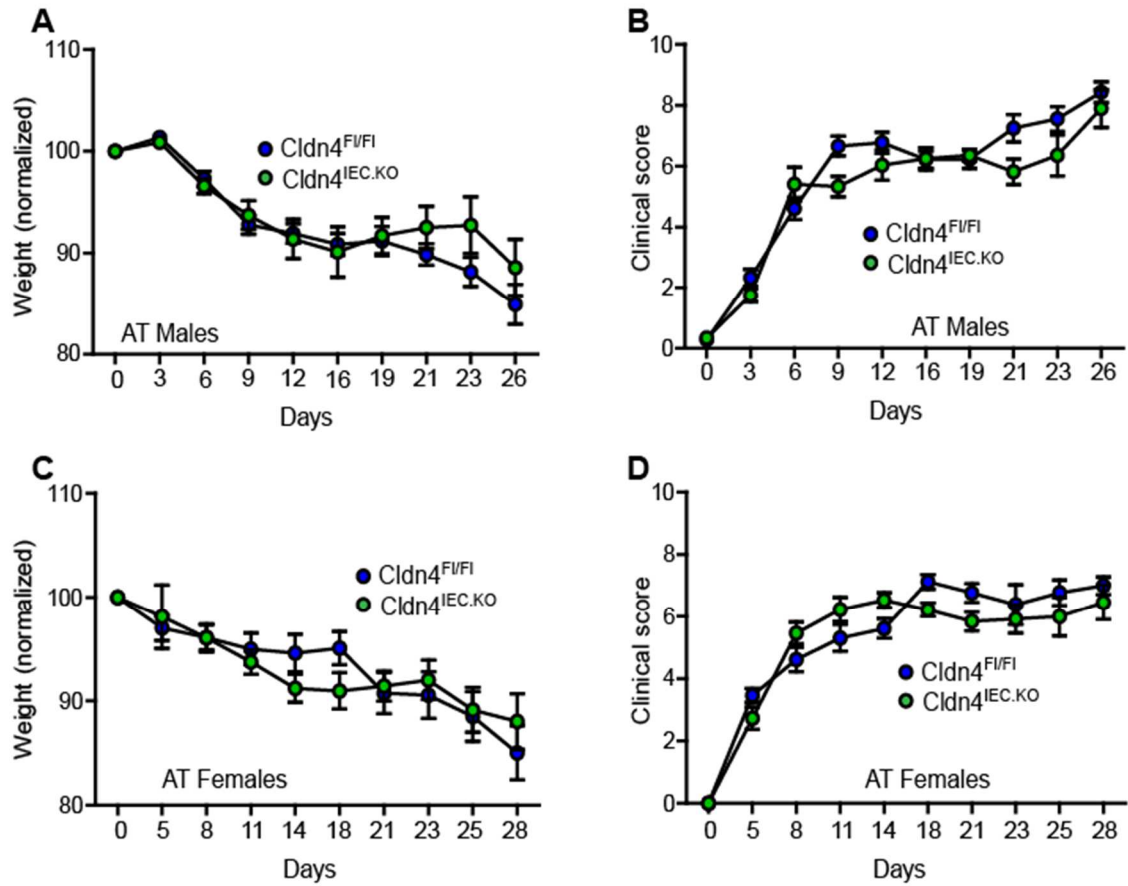
Figure 5. CLDN4$^{Fl/Fl}$ and CLDN4$^{IEC.KO}$ results in T cell transfer experimental model. A. Weight loss and **B**. clinical score comparison for CLDN4$^{IEC.KO}$ (green circles) and CLDN4$^{Fl/Fl}$ male mice (blue circles). n=12 for CLDN4$^{IEC.KO}$ and n=18 for CLDN4$^{Fl/Fl}$. **C**. Weight loss and **D**. clinical score comparison for CLDN4$^{IEC.KO}$ (green circles) and CLDN4$^{Fl/Fl}$ female mice (blue circles). n=13 per genotype.

Figure 6. AT experimental CLDN4$^{\text{IEC.KO}}$, CLDN4$^{\text{Fl/Fl}}$ and control colon samples.
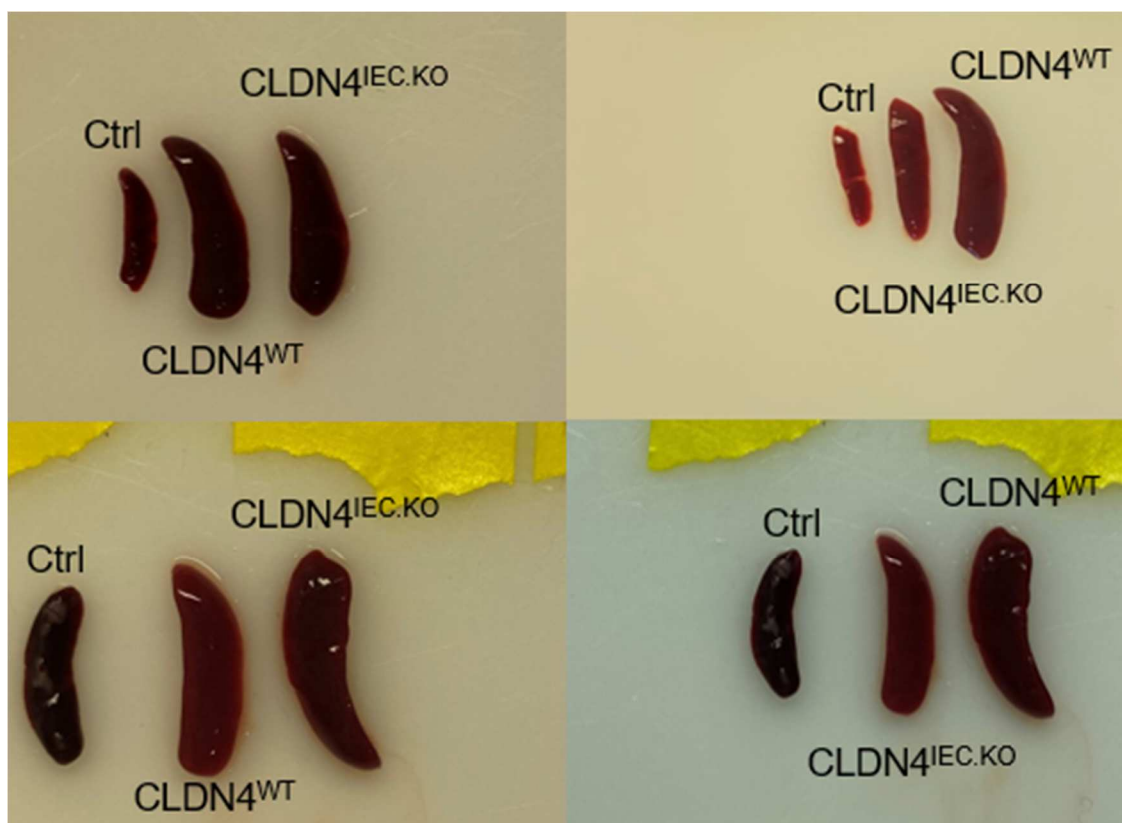
Figure 7. Spleen from CLDN4^{IEC.KO}, CLDN4^{Fl/Fl} and control AT samples.

Acute colitis experimental model on CLDN4^IEC.KO^ and CLDN4^Fl/Fl^ mice

Since the conditional claudin-4 knockout mice did not increase the disease severity in the T cell transfer experimental model, we modified our hypothesis to see if CLDN4^IEC.KO^ mice will be more protective than CLDN4^Fl/Fl^ mice. Therefore, I decided to look into the acute colitis experimental model DSS instead to see if there would be a more significant difference in CLDN4^Fl/Fl^ mice's early disease phase than the CLDN4^IEC.KO^ mice.

The disease is more severe in the female CLDN4^Fl/Fl^ mice with 1% DSS than in CLDN4^IEC.KO^ mice. As expected, the mice did not have a big difference in disease between the first six days of the experiment with 1% DSS. However, as time progressed, CLDN4Fl/Fl mice lost weight and had higher clinical scores than the CLDN4IEC.KO mice with the most significant difference on day 8. This is supported by the dramatic weight decrease between days 6-8 (**Figure 8C**) and higher disease severity peaks on day 8 (**Figure 8D**). The disease severity difference with 2% DSS between the CLDN4^Fl/Fl^ and the CLDN4^IEC.KO^ mice are insignificant, shown by the weight loss (**Figure 8E**) and clinical scores (**Figure 8F**), with the CLDN4^Fl/Fl^ mice only slightly sicker than the CLDN4^IEC.KO^ mice. The CLDN4^Fl/Fl^ mice that received 3% DSS are more diseased than the CLDN4^IEC.KO^ mice. This was demonstrated by the more significant weight loss (**Figure 8A**) and higher disease scores (**Figure 8B**). However, the disease's progression and severity were rapid and deadly for CLDN4^Fl/Fl^ and CLDN4^IEC.KO^ mice and the majority of the mice died after nine days. The CLDN4^Fl/Fl^ colon becomes more

inflamed and shorter than the CLDN4$^{IEC.KO}$ mice colon (**Figure 9**) and all

CLDN4$^{Fl/Fl}$ spleens are more inflamed than the CLDN4$^{IEC.KO}$ spleens (**Figure 10**)

were observed when these mice were sacrificed at the humane endpoint.

Consistent with the increased disease severity, IFN-γ (**Figure 13A**) and Foxp3

(**Figure 13C**) increased in CLDN4$^{Fl/Fl}$ mice relative to CLDN4$^{IEC.KO}$ mice and the

ST2+ receptors are decreased in the CLDN4$^{Fl/Fl}$ mice compared to CLDN4$^{IEC.KO}$

mice(**Figure 13B**). Overall, this data supports our modified hypothesis that in

both female and male experimental models, the CLDN4$^{IEC.KO}$ mice protect the

mice from the disease compared with the CLDN4$^{Fl/Fl}$ mice with different
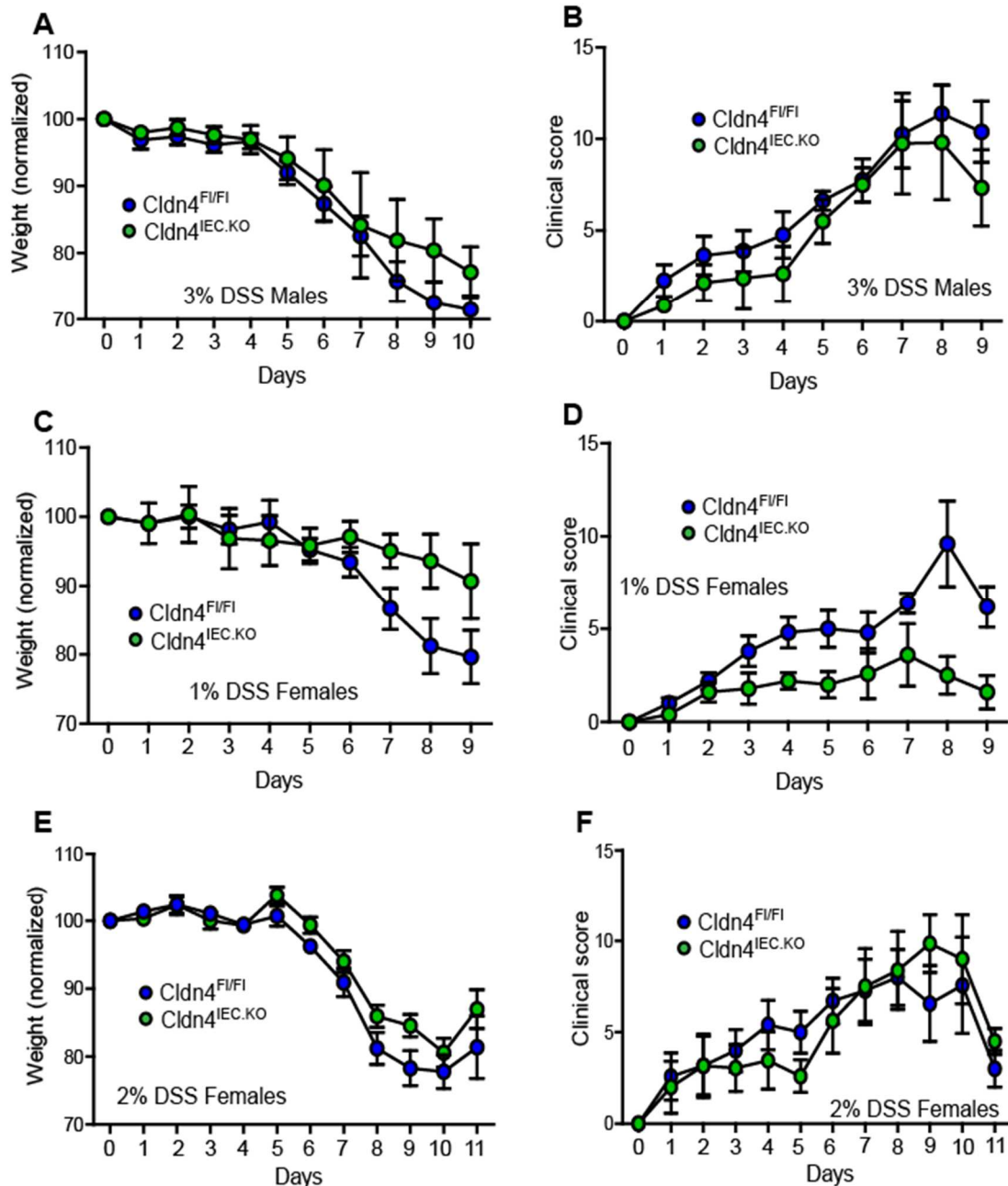
percentages of DSS.

Figure 8. CLDN4[IEC.KO] and CLDN4[Fl/Fl] results in DSS. A. Weight loss and **B**. clinical score comparison for CLDN4[IEC.KO] (green circles) and CLDN4[Fl/Fl] male mice (blue circles) with 3% DSS in water. n=8 per genotype. **C**. Weight loss and **D**. clinical score comparison for CLDN4[IEC.KO] (green circles) and CLDN4[Fl/Fl] female mice (blue circles) with 1% DSS in water. n=5 per genotype. **E**. Weight loss and **F**. clinical score comparison for CLDN4[IEC.KO] (green circles) and CLDN4[Fl/Fl] female mice (blue circles) with 2% DSS in water. n=11 for CLDN4[IEC.KO] and n=10 for CLDN4[Fl/Fl].

Figure 9. Comparison of CLDN4$^{IEC.KO}$ and CLDN4$^{Fl/Fl}$ colon in DSS.

Figure 10. Spleen from CLDN4$^{IEC.KO}$ and CLDN4$^{Fl/Fl}$ mice in DSS.

Acute colitis experimental model on CLDN4^{Tg} and CLDN4^{WT} mice

Since the CLDN4$^{Fl/Fl}$ mice have more significant disease severity than the CLDN4$^{IEC.KO}$ mice, we hypothesized that overexpression of claudin-4 will increase the disease severity more than in the CLDN4$^{Fl/Fl}$ mice. To test out the hypothesis, transgenic mice expressing mCherry-tagged mouse claudin-4 were characterized.

Since we hypothesized CLDN4^{Tg} mice would increase the disease severity, we wanted to know if claudin-4 is related to the injury or recovery phase of the disease. We hypothesized that CLDN4^{Tg} mice would undergo recovery slower than CLDN4^{WT} mice. To test this hypothesis, 2% DSS was given to CLDN4^{WT} and CLDN4^{Tg} mice for eight days and then removed DSS to monitor their recovery. The disease severity increased in the CLDN4^{Tg} mice slower than in the CLDN4^{WT} mice. This is indicated by the weight loss (**Figure 11A**) and the clinical scores (**Figure 11B**) of the CLDN4^{Tg} mice compared to the CLDN4^{WT} mice. However, after DSS withdrawal, the CLDN4^{Tg} mice had greater weight loss and higher clinical scores. Even though the weight loss difference between the two genotypes was not significant, there was a more considerable difference in the weight during recovery. The more significant difference was that the recovery rate was slower in the CLDN4^{Tg} mice, and the number of death was higher in the CLDN4^{Tg} mice (**Figure 11**). In contrast, the CLDN4^{WT} mice fully recovered, and the CLDN4^{Tg} mice did not. These data indicate that the CLDN4^{Tg} mice get higher disease severity scores and recover slower than the CLDN4^{WT} mice.

The disease severity in 1% DSS male mice is similar in CLDN4^{Tg} mice compared to CLDN4^{WT} mice. This is supported by the similar weight loss after day 6 (**Figure 12A**) and clinical scores after day 5 (**Figure 12B**) of the CLDN4^{Tg} mice. The disease severity difference of 1% DSS in female mice between the CLDN4^{Tg} and the CLDN4^{WT} mice is insignificant, shown by the weight loss (**Figure 12C**) and clinical scores (**Figure 12D**), with the CLDN4^{Tg} mice only slightly sicker than the CLDN4^{WT} mice. The weight loss (**Figure 12E**) and score (**Figure 12F**) for the 2% DSS experiment indicated that the CLDN4^{Tg} mice were slightly sicker than the CLDN4^{WT} mice, which means that the DSS had a more effect on the CLDN4^{Tg} mice than the CLDN4^{WT} mice.

However, IFN-γ (**Figure 13A**) and Foxp3 **(Figure 13C)** increased in CLDN4^{Tg} mice relative to CLDN4^{WT} mice, and the ST2^{+} receptors are decreased in the CLDN4^{Tg} mice compared to CLDN4^{WT} mice(**Figure 13B**). Based on the analysis and the long DSS experiment, the data support the hypothesis that in both female and male experimental models, the CLDN4^{Tg} mice increase the severity of experimental IBD compared to CLDN4^{WT} mice.
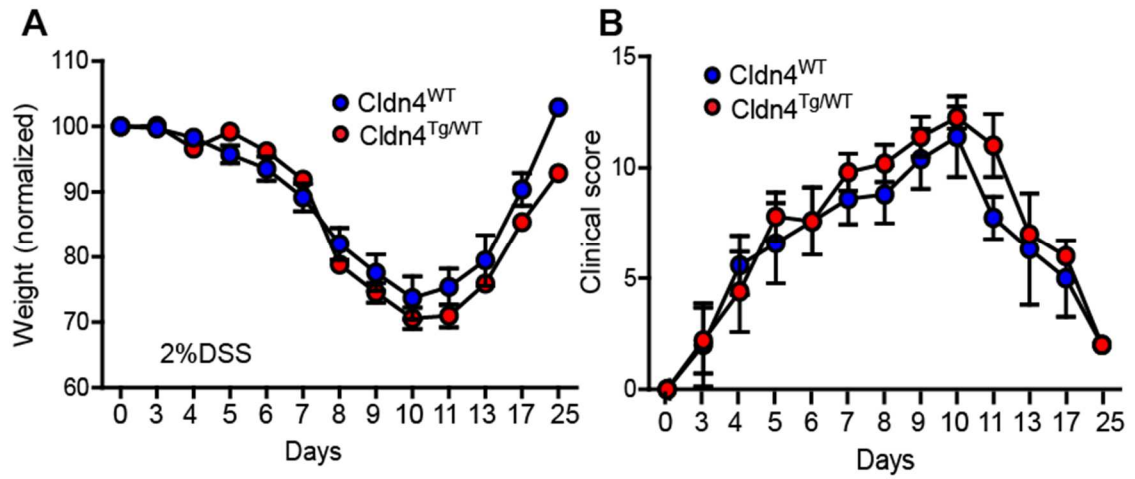
Figure 11. CLDN4^{Tg} and CLDN4^{WT} recovery after 2% DSS. A. Weight loss and **B.** clinical score comparison for CLDN4^{Tg} (red circles) and CLDN4^{WT} male mice (blue circles) with 2% DSS in water. n=5 per genotype.
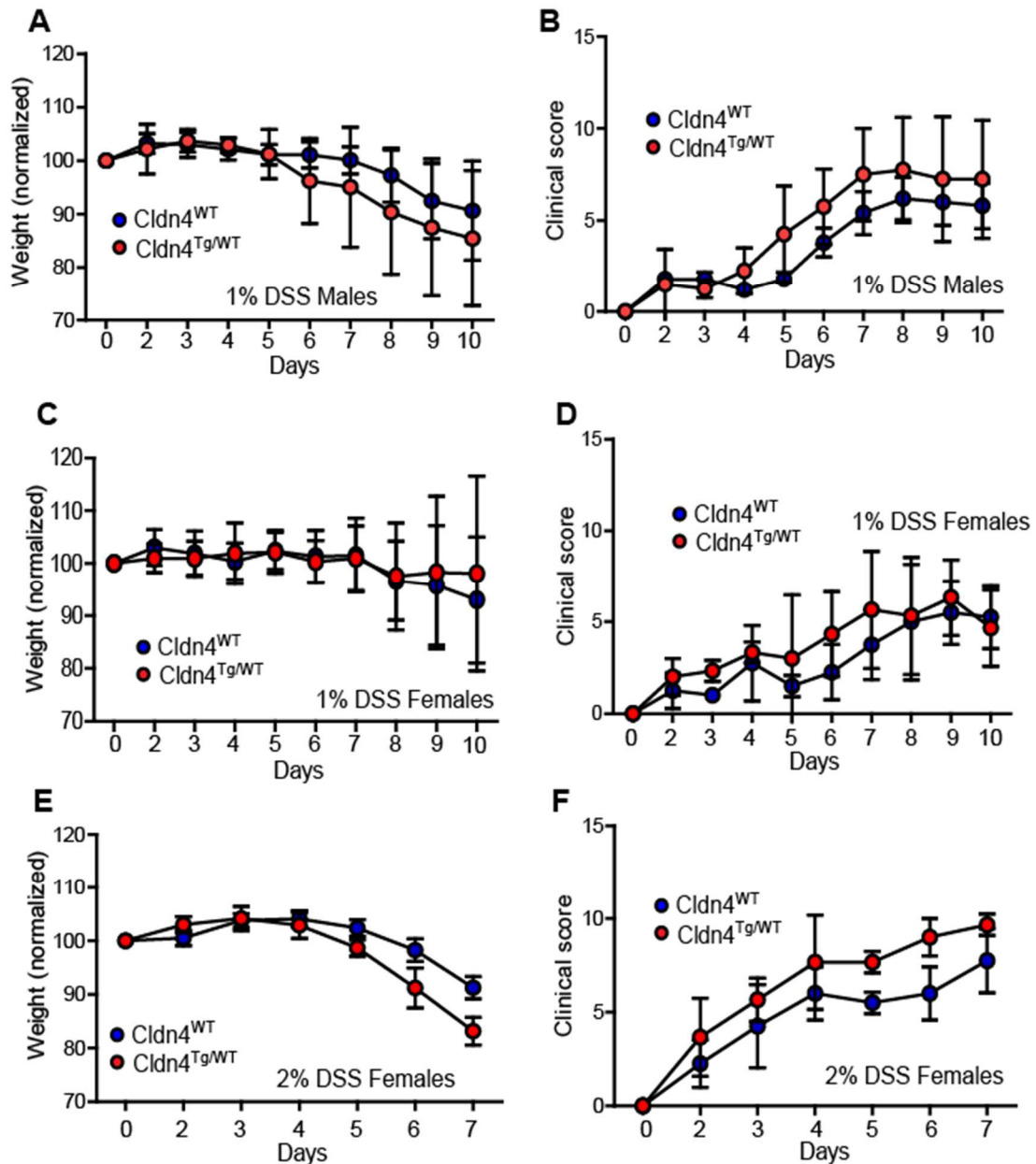
Figure 12. CLDN4^Tg and CLDN4^WT result in DSS. A. Weight loss and **B**. clinical score comparison for CLDN4^Tg (red circles) and CLDN4^WT male mice (blue circles) with 2% DSS in water. n=4 for CLDN4^Tg and n=5 for CLDN4^WT. **C**. Weight loss and **D**. clinical score comparison for CLDN4^Tg (red circles) and CLDN4^WT female mice (blue circles) with 1% DSS in water. n=3 for CLDN4^Tg and n=4 for CLDN4^WT. **E**. Weight loss and **F**. clinical score comparison for CLDN4^Tg (red circles) and CLDN4^WT female mice (blue circles) with 2% DSS in water. n=3 for CLDN4^Tg and n=4 for CLDN4^WT.
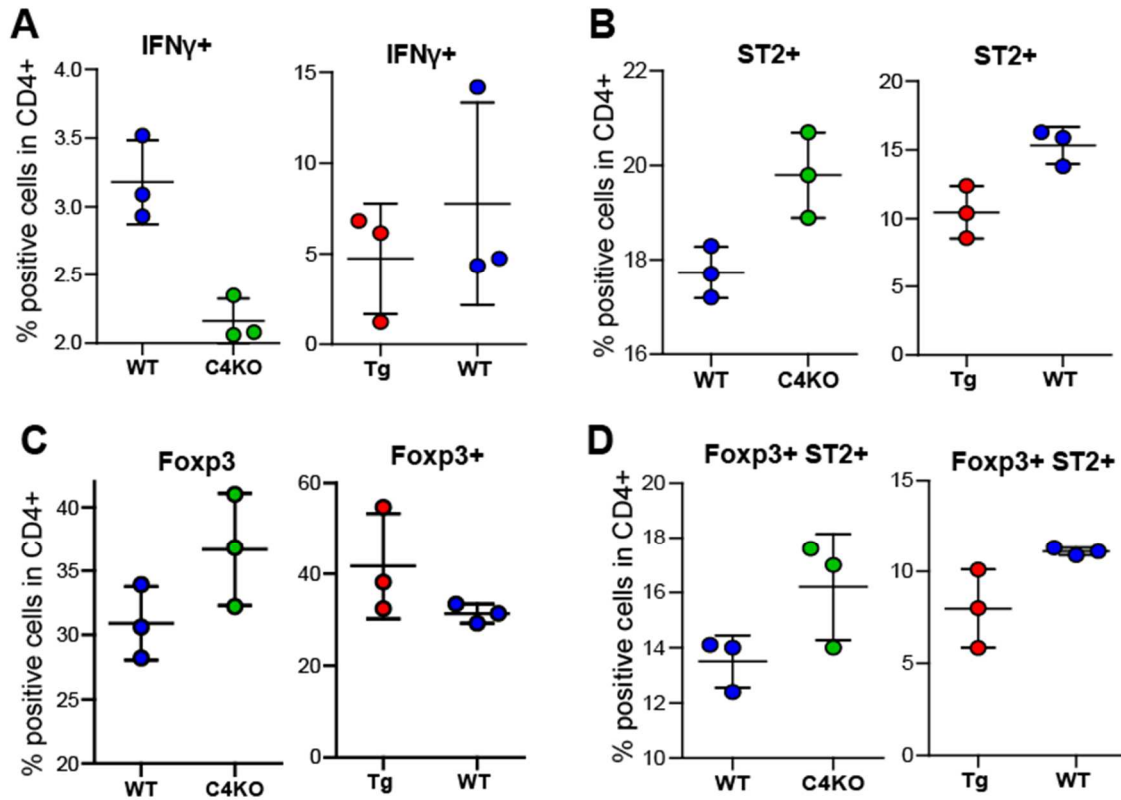
Figure 13. ST2+ levels are higher in CLDN4$^{IEC.KO}$ samples. A. IFN-γ is lower in CLDN4$^{IEC.KO}$ compared to CLDN4^{Tg} and CLDN4^{WT}. **B.** ST2+ levels for CLDN4^{WT} mice is higher than CLDN4^{Tg} mice, and highest in CLDN4$^{IEC.KO}$ mice. **C**. Foxp3 is slightly higher on CLDN4$^{IEC.KO}$ but highest in CLDN4^{Tg}. **D.** Foxp3/ST2+ levels increases from CLDN4^{Tg} to CLDN4^{WT} and to CLDN4$^{IEC.KO}$ mice.

DISCUSSION

Claudin-4, a barrier-forming claudin, is thought to enhance barrier function and could thus be beneficial in an IBD-like environment. We hypothesized that intestinal damage would increase from a loss of barrier from chronic colitis. An adoptive transfer model of colitis was established to mimic IBD. Surprisingly, CLDN4$^{IEC.KO}$ mice had less disease severity than the CLDN4$^{Fl/Fl}$ mice and the death rate of the CLDN4$^{IEC.KO}$ mice are lower than the CLDN4$^{Fl/Fl}$ mice. The severity of the disease caused more inflamed colon and spleens in the CLDN4$^{Fl/Fl}$. These results suggest that CLDN4$^{IEC.KO}$ is protecting because the disease progression is slower than CLDN4$^{Fl/Fl}$. This was surprising because this suggests that claudin-4 has a function in barrier protection and maybe a secondary function in wound repair.

The results of the adoptive transfer experiment suggest that CLDN4$^{Fl/Fl}$ mice have the ability to cause injury. A DSS model was established to mimic epithelial injury for its reproducibility and rapidity. Similar to the AT model, the spleens and colons of the CLDN4$^{Fl/Fl}$ are more inflamed in the colon and the spleen. Unexpectedly, there was only a slight difference in the weight and the clinical scores between the two genotypes with 3% DSS even though the CLDN4$^{Fl/Fl}$ mice develop disease sooner than the CLDN4$^{IEC.KO}$ mice, the disease severity in the CLDN4$^{IEC.KO}$ would increase near the end of the experiment. The 3% DSS likely became too harmful to the recipients, causing almost all the mice from both CLDN4$^{IEC.KO}$ and CLDN4$^{Fl/Fl}$ groups died on day 9. Intestinal damage

caused by the 2% DSS results was inconclusive, most likely due to the harmful effect of DSS that causes the disease to develop around the same time for both CLDN4$^{IEC.KO}$ and CLDN4$^{Fl/Fl}$. Recent studies have shown that IL-33/ST2 is an essential factor in the beginning disease phase and later on during the recovery phase of the disease [94]. Although it was not significant due to the number of recipients, there were more ST2 receptors in CLDN4$^{IEC.KO}$ mice compared to the CLDN4$^{Fl/Fl}$ mice. IFN-γ is produced by immune cells and plays an important role in antimicrobial responses. There are also fewer IFN-γ expressing cells in the CLDN4$^{IEC.KO}$ mice compared to the CLDN4$^{Fl/Fl}$ mice. These findings support the previous models that the CLDN4$^{Fl/Fl}$ mice have higher disease severity than the CLDN4$^{IEC.KO}$ mice.

Since conditionally knocking out claudin-4 will reduce the disease severity, we hypothesized that the overexpression of claudin-4 will increase the disease severity. Therefore, CLDN4^{Tg} mice were produced in the lab and tested for fluorescence for CLDN4^{Tg} signals before the experiment. Despite our hypothesis, the difference in weight and disease was negligible between the two genotypes. However, weight was lower, and the disease severity was slightly higher for CLDN4^{Tg} mice than CLDN4^{WT}. The data also indicates that the CLDN4^{Tg} mice recover slower than the CLDN4^{WT} mice, with fewer mice surviving to the end. These findings suggest that the CLDN4^{Tg} mice are slower in the recovery phase of the disease and can cause them to die before full recovery. To further investigate the disease, our studies focused on the initial phase of the disease.

As expected, the disease severity in CLDN4^{Tg} mice was higher than in the CLDN4^{WT} mice with 1% DSS. Based on the results, it did not show a significant difference between the two genotypes. However, the CLDN4^{Tg} mice became slightly sicker based on the symptoms of DSS, consisting of weight loss, hunched posture, decreased activity, and blood in the stool. Surprisingly, the results from the 2% DSS female mice showed a clear distinction between the progression of disease between CLDN4^{Tg} and CLDN4^{WT} mice. From our data, there are more ST2 receptors in CLDN4^{WT} compared to the CLDN4^{Tg} mice. The results also showed fewer IFN-γ expressing cells in the CLDN4^{WT} mice than in the CLDN4^{Tg} mice. Overall, our results suggest that IL-33/ST2 protects the mice from disease and causes less IFN-γ recruitment to the disease site. Since the DSS model acts by causing direct injury to intestinal epithelia, claudin-4 may play a secondary role that deals with cell migration and restitution.

CONCLUSIONS

In this study, we used several models of experimental IBD to show that CLDN4^{Tg} and CLDN4^{WT}, not CLDN4$^{IEC.KO}$ caused higher disease severity in mice. This was both unexpected and novel, since claudin-4 is consider to be an epithelial barrier-protective claudin, whereby loss of claudin-4 should have exacerbated disease. Since DSS colitis closely replicates epithelial injury model, it is likely that claudin-4 knockouts compensate for injury by accelerating either cell proliferation or cell migration, which will be investigated in the future.

BIBLIOGRAPHY

1.   Franzosa, E.A., et al., *Gut microbiome structure and metabolic activity in inflammatory bowel disease.* Nature Microbiology, 2019. **4**(2): p. 293-305.

2.   Nalle, S.C., et al., *Graft-versus-host disease propagation depends on increased intestinal epithelial tight junction permeability.* Journal of Clinical Investigation, 2019. **129**(2): p. 902-914.

3.   Graham, W.V., et al., *Intracellular MLCK1 diversion reverses barrier loss to restore mucosal homeostasis.* Nature Medicine, 2019. **25**(4): p. 690-700.

4.   Abraham, C. and J.H. Cho, *Inflammatory bowel disease.* New England Journal of Medicine, 2009. **361**(21): p. 2066-78.

5.   Bischoff, S.C., et al., *Intestinal permeability – a new target for disease prevention and therapy.* BMC Gastroenterology, 2014. **14**(1): p. 189.

6.   Jenkins, R.T., et al., *Reversibility of increased intestinal permeability to 51Cr-EDTA in patients with gastrointestinal inflammatory diseases.* American Journal of Gastroenterol, 1987. **82**(11): p. 1159-64.

7.   Jenkins, R.T., et al., *Small bowel and colonic permeability to 51Cr-EDTA in patients with active inflammatory bowel disease.* Clinical and Investigative Medicine, 1988. **11**(2): p. 151-5.

8.   Peeters, M., et al., *Increased permeability of macroscopically normal small bowel in Crohn's disease.* Digestive Diseases and Sciences, 1994. **39**(10): p. 2170-6.

9.   Peeters, M., et al., *Clustering of increased small intestinal permeability in families with Crohn's disease.* Gastroenterology, 1997. **113**(3): p. 802-7.

10.   Edelblum, K.L. and J.R. Turner, *Epithelial Cells: Structure, Transport, and Barrier Function*, in *Mucosal Immunology*, M.W. Russell, et al., Editors. 2015, Elsevier. p. 187-210.

11.   Sato, T., et al., *Single Lgr5 stem cells build crypt-villus structures in vitro without a mesenchymal niche.* Nature, 2009. **459**: p. 262-5.

12.   Wang, Y., et al., *Long-Term Culture Captures Injury-Repair Cycles of Colonic Stem Cells.* Cell, 2019. **179**(5): p. 1144-1159 e15.

13. Haegebarth, A. and H. Clevers, *Wnt signaling, lgr5, and stem cells in the intestine and skin.* American Journal of Pathology, 2009. **174**(3): p. 715-21.

14. Bry, L., et al., *Paneth cell differentiation in the developing intestine of normal and transgenic mice.* Proceedings of the National Academy of Sciences of the United States of America, 1994. **91**(22): p. 10335-9.

15. Hansson, G.C. and M.E. Johansson, *The inner of the two Muc2 mucin-dependent mucus layers in colon is devoid of bacteria.* Gut Microbes, 2010. **1**(1): p. 51-54.

16. Banerjee, A., et al., *Interpreting heterogeneity in intestinal tuft cell structure and function.* Journal of Clinical Investigation, 2018. **128**(5): p. 1711-1719.

17. Paulus, U., et al., *The differentiation and lineage development of goblet cells in the murine small intestinal crypt: experimental and modelling studies.* Journal of Cell Science, 1993. **106 (Pt 2)**: p. 473-83.

18. Nowarski, R., R. Jackson, and R.A. Flavell, *The Stromal Intervention: Regulation of Immunity and Inflammation at the Epithelial-Mesenchymal Barrier.* Cell, 2017. **168**(3): p. 362-375.

19. Gerbe, F., et al., *Intestinal epithelial tuft cells initiate type 2 mucosal immunity to helminth parasites.* Nature, 2016. **529**(7585): p. 226-30.

20. Howitt, M.R., et al., *Tuft cells, taste-chemosensory cells, orchestrate parasite type 2 immunity in the gut.* Science, 2016.

21. McKinley, E.T., et al., *Optimized multiplex immunofluorescence single-cell analysis reveals tuft cell heterogeneity.* JCI Insight, 2017. **2**(11).

22. Haber, A.L., et al., *A single-cell survey of the small intestinal epithelium.* Nature, 2017. **551**(7680): p. 333-339.

23. Lueschow SR, McElroy SJ. *The Paneth Cell: The Curator and Defender of the Immature Small Intestine.* Frontiers in Immunology, 2020.11:587.

24. Ukabam, S.O., J.R. Clamp, and B.T. Cooper, *Abnormal small intestinal permeability to sugars in patients with Crohn's disease of the terminal ileum and colon.* Digestion, 1983. **27**(2): p. 70-4.

25. Turner, J.R., Intestinal mucosal barrier function in health and disease. Nature Reviews Immunology, 2009. 9(11): p. 799-809.

26. Kong, C.T., A. Varde, and J.E. Lever, *Targeting of recombinant Na+/glucose cotransporter (SGLT1) to the apical membrane.* FEBS Letters, 1993. **333**(1-2): p. 1-4.

27. Turk, E., M.G. Martin, and E.M. Wright, *Structure of the human Na+/glucose cotransporter gene SGLT1.* Journal of Biological Chemistry, 1994. **269**(21): p. 15204-9.

28. Saha, P., et al., *Molecular mechanism of regulation of villus cell Na-K-ATPase in the chronically inflamed mammalian small intestine.* Biochimica et Biophysica Acta, 2015. **1848**(2): p. 702-11.

29. Turner, J.R., *Epithelia and gastrointestinal function*, in *Yamada's Textbook of Gastroenterology*, D.K. Podolsky, et al., Editors. 2016, John Wiley & Sons. p. 317-329.

30. Shen, L., et al., *Tight junction pore and leak pathways: a dynamic duo.* Annual Review of Physiology, 2011. **73**: p. 283-309.

31. Yu, M., et al., *Nononcogenic restoration of the intestinal barrier by E. coli-delivered human EGF.* JCI Insight, 2019. **4**(16).

32. Van Itallie, C.M., et al., *The density of small tight junction pores varies among cell types and is increased by expression of claudin-2.* Journal of Cell Science, 2008. **121**(Pt 3): p. 298-305.

33. Van Itallie, C.M. and J.M. Anderson, *Claudins and epithelial paracellular transport.* Annual Review of Physiology, 2006. **68**: p. 403-29.

34. Yu, A.S., *Claudins and the kidney.* J Am Soc Nephrol, 2015. **26**(1): p. 11-9. Journal of the American Society of Nephrology

35. Turksen, K. and T.C. Troy, *Permeability barrier dysfunction in transgenic mice overexpressing claudin 6.* Development, 2002. **129**(7): p. 1775-84.

36. Sasaki, H., et al., *Dynamic behavior of paired claudin strands within apposing plasma membranes.* Proceedings of the National Academy of Sciences of the United States of America, 2003. **100**(7): p. 3971-6.

37.   Krug, S.M., et al., *Tricellulin forms a barrier to macromolecules in tricellular tight junctions without affecting ion permeability.* Molecular Biology of the Cell, 2009. **20**(16): p. 3713-24.

38.   Turner, J.R., et al., *Physiological regulation of epithelial tight junctions is associated with myosin light-chain phosphorylation.* American Journal of Physiology, 1997. **273**(4): p. C1378-85.

39.   Odenwald, M.A. and J.R. Turner, *The intestinal epithelial barrier: a therapeutic target?* Nature Reviews Gastroenterology & Hepatology, 2017. **14**(1): p. 9-21.

40.   Zuo, L., W.T. Kuo, and J.R. Turner, *Tight Junctions as Targets and Effectors of Mucosal Immune Homeostasis.* Cellular and Molecular Gastroenterology and Hepatology, 2020. **10**(2): p. 327-340.

41.   Buschmann MM, Shen L, Rajapakse H, et al. *Occludin OCEL-domain interactions are required for maintenance and regulation of the tight junction barrier to macromolecular flux.* Molecular Biology of the Cell, 2013. 24(19):3056-3068.

42.   Wang, F., et al., *Interferon-gamma and tumor necrosis factor-alpha synergize to induce intestinal epithelial barrier dysfunction by up-regulating myosin light chain kinase expression.* The American Journal of Pathology, 2005. **166**(2): p. 409-19.

43.   Umeda, K., et al., *ZO-1 and ZO-2 independently determine where claudins are polymerized in tight-junction strand formation.* Cell, 2006. **126**(4): p. 741-54.

44.   Otani, T., et al., *Claudins and JAM-A coordinately regulate tight junction formation and epithelial polarity.* Journal of Cell Biology, 2019. **218**(10): p. 3372-3396.

45.   Chassaing, B., et al., *Dextran sulfate sodium (DSS)-induced colitis in mice.* Current Protocols in Immunology, 2014. **104**: p. Unit 15 25.

46.   Morampudi, V., et al., *DNBS/TNBS colitis models: providing insights into inflammatory bowel disease and effects of dietary fat.* Journal of Visualized Experiments, 2014(84): p. e51297.

47.   Pongkorpsakol P, Turner JR, Zuo L. *Culture of Intestinal Epithelial Cell Monolayers and Their Use in Multiplex Macromolecular Permeability*

Assays for In Vitro Analysis of Tight Junction Size Selectivity. Current Protocols in Immunology, 2020. 131(1):e112.

48. Amasheh, S., et al., *Claudin-2 expression induces cation-selective channels in tight junctions of epithelial cells.* Journal of Cell Science, 2002. **115**(Pt 24): p. 4969-76.

49. Krause, G., et al., *Structure and function of claudins.* Biochimica et Biophysica Acta, 2008. **1778**(3): p. 631-45.

50. Krug, S.M., et al., *Charge-selective claudin channels.* Annals of the New York Academy of Sciences, 2012. **1257**: p. 20-8.

51. Angelow, S. and A.S. Yu, Cysteine mutagenesis to study the structure of claudin-2 paracellular pores. Annals of the New York Academy of Sciences, 2009. 1165: p. 143-7.

52. Li, J., et al., Claudin-2 pore function requires an intramolecular disulfide bond between two conserved extracellular cysteines. American Journal of Physiology-Cell Physiology, 2013. 305(2): p. C190-6.

53. Li, J., et al., Conserved aromatic residue confers cation selectivity in claudin-2 and claudin-10b. Journal of Biological Chemistry, 2013. 288(31): p. 22790-7.

54. Yu, A.S., et al., Molecular basis for cation selectivity in claudin-2-based paracellular pores: identification of an electrostatic interaction site. The Journal of General Physiology, 2009. 133(1): p. 111-27.

55. Suzuki, H., et al., Crystal structure of a claudin provides insight into the architecture of tight junctions. Science, 2014. 344(6181): p. 304-7.

56. Hou J, Renigunta A, Yang J, Waldegger S. Claudin-4 forms paracellular chloride channel in the kidney and requires claudin-8 for tight junction localization. Proceedings of the National Academy of Sciences of the United States of America. 2010;107(42):18010-18015.

57. Krug SM, et al., *Claudin-17 forms tight junction channels with distinct anion selectivity.* Cellular and Molecular Life Sciences, 2012. 69(16):2765-78.

58. Rosenthal R, Milatz S, Krug SM, et al. *Claudin-2, a component of the tight junction, forms a paracellular water channel.* Journal of Cell Science. 2010;123(Pt 11):1913-1921.

59.   Van Itallie CM, Rogan S, Yu A, Vidal LS, Holmes J, Anderson JM. *Two splice variants of claudin-10 in the kidney create paracellular pores with different ion selectivities.* American Journal of Physiology - Renal Physiology. 2006;291(6):F1288-F1299.

60.   Günzel D, Yu A.S., *Claudins and the modulation of tight junction permeability.* Physiological Reviews, 2013. 93(2):525-69.

61.   Katahira J, Inoue N, Horiguchi Y, Matsuda M, Sugimoto N. *Molecular cloning and functional characterization of the receptor for Clostridium perfringens enterotoxin.* Journal of Cell Biology. 1997.136(6):1239-1247.

62.   Katahira J, Sugiyama H, Inoue N, Horiguchi Y, Matsuda M, Sugimoto N. *Clostridium perfringens enterotoxin utilizes two structurally related membrane proteins as functional receptors in vivo.* Journal of Biological Chemistry, 1997.272(42):26652-26658.

63.   Findley, M.K. and Koval, M., *Regulation and roles for claudin-family tight junction proteins.* IUBMB Life, 2009. 61: 431-437.

64.   Kirk A, et al., Differential expression of claudin tight junction proteins in the human cortical nephron. Nephrology Dialysis Transplantation, 2010. 25: 2107–2119.

65.   Kiuchi-Saishin Y, et al., *Differential expression patterns of claudins, tight junction membrane proteins, in mouse nephron segments.* Journal of the American Society of Nephrology, 2002. 13(4):875-886.

66.   Fujita H, Chiba H, Yokozaki H, et al. *Differential Expression and Subcellular Localization of Claudin-7, −8, −12, −13, and −15 Along the Mouse Intestine.* Journal of Histochemistry & Cytochemistry, 2006. 54(8):933-944

67.   Holmes JL, Van Itallie CM, Rasmussen JE, Anderson JM. *Claudin profiling in the mouse during postnatal intestinal development and along the gastrointestinal tract reveals complex expression patterns.* Gene Expression Patterns. 2006. 6(6):581-8.

68.   Rahner C, Mitic LL, Anderson JM. *Heterogeneity in expression and subcellular localization of claudins 2, 3, 4, and 5 in the rat liver, pancreas, and gut.* Gastroenterology. 2001. 120(2):411-422.

69. Peng S, Adelman RA, Rizzolo LJ. *Minimal effects of VEGF and anti-VEGF drugs on the permeability or selectivity of RPE tight junctions*. Investigative Ophthalmology & Visual Science. 2010. 51(6):3216-3225.

70. Colegio OR, Van Itallie CM, McCrea HJ, Rahner C, Anderson JM. *Claudins create charge-selective channels in the paracellular pathway between epithelial cells.* American Journal of Physiology-Cell Physiology. 2002;283(1):C142-C147.

71. Turpin, W., et al., *Analysis of Genetic Association of Intestinal Permeability in Healthy First-degree Relatives of Patients with Crohn's Disease.* Inflammatory Bowel Diseases, 2019. **25**(11): p. 1796-1804.

72. Hollander, D., et al., *Increased intestinal permeability in patients with Crohn's disease and their relatives. A possible etiologic factor.* Annals of Internal Medicine, 1986. **105**(6): p. 883-5.

73. Soderholm, J.D., et al., *Different intestinal permeability patterns in relatives and spouses of patients with Crohn's disease: an inherited defect in mucosal defence?* Gut, 1999. **44**(1): p. 96-100.

74. Hollander, D., *Permeability in Crohn's disease: altered barrier functions in healthy relatives?* Gastroenterology, 1993. **104**(6): p. 1848-51.

75. May, G.R., L.R. Sutherland, and J.B. Meddings, *Is small intestinal permeability really increased in relatives of patients with Crohn's disease?* Gastroenterology, 1993. **104**(6): p. 1627-32.

76. Poritz LS, Harris LR, Kelly AA, Koltun WA. *Increase in the tight junction proteinclaudin-1 in intestinal inflammation.* Digestive Diseases and Sciences, 2011;56:2802–9.

77. Weber CR, Nalle SC, Tretiakova M, Rubin DT, Turner JR. *Claudin-1 and claudin-2 expression is elevated in inflammatory bowel disease and may contributeto early neoplastic transformation.* Laboratory Investigation, 2008. 88:1110–20.

78. Garcia-Hernandez V, Quiros M, Nusrat A. *Intestinal epithelial claudins: expression and regulation in homeostasis and inflammation.* Annals of the New York Academy of Sciences, 2017. 1397:66–79.

79. Zeissig S, Bürgel N, Günzel D, Richter J, Mankertz J, Wahnschaffe U, et al. *Changes in expression and distribution of claudin 2, 5 and 8 lead to*

discontinuous tight junctions and barrier dysfunction in active Crohn's disease. Gut, 2007;56:61–72.

80. Goswami P, Das P, Verma AK, Prakash S, Das TK, Nag TC, et al. *Are alterations of tight junctions at molecular and ultrastructural level different in duodenal biopsies of patients with celiac disease and Crohn's disease?* Virchows Archiv, 2014. 465:521–30.

81. Fischer A, Gluth M, Weege F, Pape UF, Wiedenmann B, Baumgart DC,et al. *Glucocorticoids regulate barrier function and claudin expression in intestinal epithelial cells via MKP-1.* American Journal of Physiology-Gastrointestinal and Liver Physiology, 2014. 306:G218–28.

82. Zeissig, S., et al., *Changes in expression and distribution of claudin 2, 5 and 8 lead to discontinuous tight junctions and barrier dysfunction in active Crohn's disease.* Gut, 2007. **56**(1): p. 61-72.

83. Schumann M, Günzel D, Buergel N, Richter JF, Troeger H, May C, et al. *Cell polarity-determining proteins Par-3 and PP-1 are involved in epithelial tight junction defects in coeliac disease.* Gut, 2012. 61:220–8.

84. Raju, P., et al., *Inactivation of paracellular cation-selective claudin-2 channels attenuates immune-mediated experimental colitis in mice.* Journal of Clinical Investigation, 2020.

85. Barmeyer C, Schulzke JD, Fromm M. *Claudin-related intestinal diseases.* Seminars in Cell and Developmental Biology, 2015. 42:30-38.

86. Oshima T, Miwa H, Joh T. *Changes in the expression of claudins in activeulcerative colitis.* Journal of Gastroenterology and Hepatology. 2008. 23(Suppl. 2):S146–50.

87. Alex P, Zachos NC, Nguyen T, et al. *Distinct cytokine patterns identified from multiplex profiles of murine DSS and TNBS-induced colitis.* Inflammatory Bowel Diseases, 2009. 15(3):341-352.

88. Chassaing, B., Aitken, J.D., Malleshappa, M. and Vijay-Kumar, M. *Dextran Sulfate Sodium (DSS)-Induced Colitis in Mice.* Current Protocols in Immunology, 2004. 104: 15.25.1-15.25.14.

89. Powrie F. *T cells in inflammatory bowel disease: protective and pathogenic roles.* Immunity, 1995. 3(2):171-174.

90.	Powrie F, Leach MW, Mauze S, Menon S, Caddle LB, Coffman RL. *Inhibition of Th1 responses prevents inflammatory bowel disease in scid mice reconstituted with CD45RBhi CD4+ T cells.* Immunity, 1994. 1(7):553-562.

91.	Ostanin DV, Bao J, Koboziev I, et al. *T cell transfer model of chronic colitis: concepts, considerations, and tricks of the trade.* American Journal of Physiology-Gastrointestinal and Liver Physiology. 2009, 296(2):G135-G146.

92.	Gong Y, Yu M, Yang J, et al. *The Cap1-claudin-4 regulatory pathway is important for renal chloride reabsorption and blood pressure regulation.* Proceedings of the National Academy of Sciences of the United States of America. 2014. 111(36):E3766-E3774.

93.	Markov, A.G., Aschenbach, J.R. and Amasheh, S. *Claudin clusters as determinants of epithelial barrier function.* IUBMB Life, 2015. 67: 29-35.

94.	Lopetuso LR, De Salvo C, Pastorelli L, et al. *IL-33 promotes recovery from acute colitis by inducing miR-320 to stimulate epithelial restitution and repair.* Proceedings of the National Academy of Sciences of the United States of America, 2018. 115(40):E9362-E9370.

CURRICULUM VITAE